A Thermodynamic Landscape of Hydrogen Cyanide-Derived Molecules and Polymers

ACS EARTH AND SPACE CHEMISTRY

http://pubs.acs.org/journal/aesccq

Article

A Thermodynamic Landscape of Hydrogen Cyanide-Derived Molecules and Polymers

Hilda Sandström, Fernando Izquierdo-Ruiz, Marco Cappelletti, Rana Dogan, Siddhant Sharma, Clara Bailey, and Martin Rahm*

Cite This: *ACS Earth Space Chem.* 2024, 8, 1272–1280

Read Online

ACCESS | Metrics & More | Article Recommendations | Supporting Information

ABSTRACT: Hydrogen cyanide (HCN)-derived molecules and polymers are featured in several hypotheses on the origin of life. Over half a century of investigations into HCN self-reactions have led to many suggestions regarding the structural nature of the products and an even greater number of proposed polymerization pathways. A comprehensive overview of possible reactions and structures is missing. In this work, we use quantum chemical calculations to map the relative Gibbs free energy of most HCN-derived molecules and polymers that have been discussed in the literature. Our computed free energies indicate that several previously considered polymerization pathways are not spontaneous and should be discarded from future consideration. Among the most thermodynamically favored products are polyaminoimidazole and adenine.

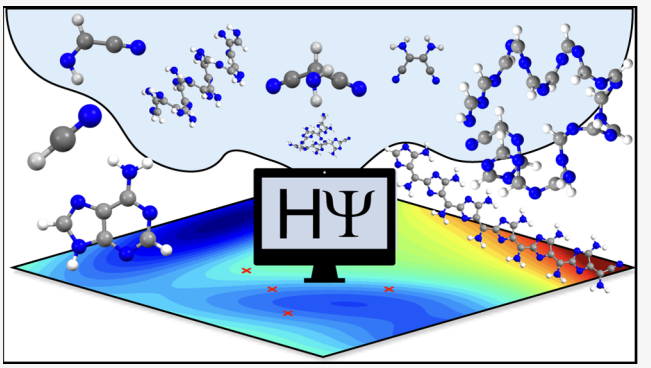

KEYWORDS: *prebiotic chemistry, iminoacetonitrile, diaminomaleonitrile, tholins, adenine, Titan*

INTRODUCTION

In this work, we use quantum chemistry to map the thermodynamic landscape of hydrogen cyanide (HCN)-derived molecules and polymers. HCN is a common molecule in the universe, having been identified on various planets,[1] dwarf planets,[2] Saturn's moon Titan,[3] comets,[4] and in the interstellar medium.[5] HCN was likely present on the early Earth.[6] The molecule is also quite reactive. In experiments, biologically relevant molecules such as amino acids, nucleobases, and pterins[7] have all been extracted from the products of HCN polymerization experiments (see ref 8 for a review).

The prevalence of HCN in many astrochemical environments, and its reactive nature, places the molecule, and its possible reaction products, at the center stage of prebiotic chemistry and astrobiology.[9,10] However, a clear picture of HCN reactivity, both in the laboratory and in astrochemical environments, remains elusive.

HCN-derived polymers are complex materials that can form under a variety of laboratory conditions.[11] These product mixtures are typically heterogeneous and insoluble in most common solvents.[12] Various forms of characterization have been attempted to elucidate which chemical structures can form from HCN. For example, mass spectrometry, infrared spectroscopy, and nuclear magnetic resonance (NMR) spectroscopy have been used to infer a wide variety of functional groups in polymerization product mixtures.[13−16] A plethora of different polymerization pathways have been proposed to explain this complexity (see ref 11 for a review). Due to their diverse nature, some HCN-derived polymers are functional materials with proposed uses in catalysis,[10,17] as adhesives and as coatings.[18,19]

The Complex Space of HCN-Derived Chemistry. For this analysis, we have collected HCN-based materials that appear as suggestions, hypotheses, or confirmed detections in the literature. The limitations of our selection are motivated by practicality. The full structural space of possible HCN-derived polymers and molecules is immense. For example, one automated search for reactions that result in HCN tetramers identified 678 compounds.[20] Several other structures have also been computationally predicted.[21] We here consider a selection of pure HCN-based materials, i.e., structures where the stoichiometries of H, C, and N are 1:1:1 (and no additional elements). Other HCN-based materials can incorporate oxygen,[11] additional nitrogen, and hydrogen[22] or form through condensation reactions, e.g., through the formation of NH_3.[11,17,23,24] Such materials, which may also

Received: April 8, 2024
Revised: May 24, 2024
Accepted: May 24, 2024
Published: June 7, 2024

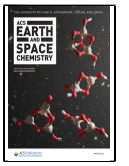

be important, are beyond the scope of this work. In the following, we will first introduce the materials we study and then proceed to evaluate their relative thermodynamic stability.

HCN-Derived Molecules. All HCN-derived molecules that we investigated are shown in Figure 1. In addition to HCN (**1**), several of these molecules have been proposed to act as monomers in polymerization:[11,13,15,25−33] the HCN dimers iminoacetonitrile (**2**) and aminocyanocarbene (**3**), the trimer aminomalononitrile (**4**), and the tetramer diaminomaleonitrile (**5**) (Figure 1). Out of these molecules, only **5** has been directly observed during polymerization of HCN.[31,34] Speculations that **2** and **4** might form are based on indirect evidence.[34] The proposed formation of **3** is controversial, as we will return to discuss. Aminoimidazole carbonitrile (**6**) and adenine (**7**) (Figure 1) are less likely to take part in polymerization but are included in our study because of their relevance to prebiotic chemistry.[11,25]

To aid our discussion, we outline a collection of pathways, which connect some of the molecules in Figure 1 to different proposed polymer structures. Sometimes, these pathways will be mentioned in the context of mechanistic details (e.g., base- or radical-catalyzed). However, we mostly use pathway to refer to the causal connections between reactant, intermediates, and products.

Suggested Products of HCN Polymerization. Two of the simplest HCN-derived polymers are polyimine (**8**) (Figure 2, pathway 1) and head-to-tail polymer (**9**) (Figure 2, pathway 2). Structures **8** and **9** have been suggested to form through different mechanisms. He et al.[15] have suggested that the formation of **8** is base-catalyzed, proceeding through the successive additions of cyanide anions. Mozhaev et al.,[32] who studied radiation-induced HCN polymerization, and Mamajanov and Herzfeld, who studied polymerization in the presence of radical initiators,[31] have both suggested **9** as a plausible product. Mamajanov and Herzfeld have further proposed that **9** can subsequently transform into two-dimensional polytriazine sheets (**10**, Figure 2). Both structures **9** and **10** have been computationally predicted to form when solid HCN is subjected to pressures above 72 GPa.[35]

Figure 3 shows **11**, the only three-dimensionally connected polymer in this study. This material can be viewed as an NN ↔ HCN substituted analogue of cubic gauche nitrogen—a metastable allotrope of nitrogen synthesized above 42 GPa.[36] Structure **11** has been predicted to be dynamically stable (a minimum on the potential energy surface).[37]

Polymerization of Iminoacetonitrile (2). Several polymers have been proposed to form from the polymerization of **2**. One such structure is Völker's ladder polymer polyaminocyanomethylene (**12**) (Figure 4, pathway 3a). In Völker's model, **12** converts to a cyclic "ladder" structure (**13**).[13] Umemoto and colleagues have suggested an alternative "single-ladder" structure (**14**) (pathway 3b).[33] Ruiz-Bermejo and colleagues have suggested that **2** may react to form structures **16** and **17** (pathways 4a and 4b).[11]

Polymerization of Diaminomaleonitrile (5). Molecule **5** features prominently in HCN reaction hypotheses because it is

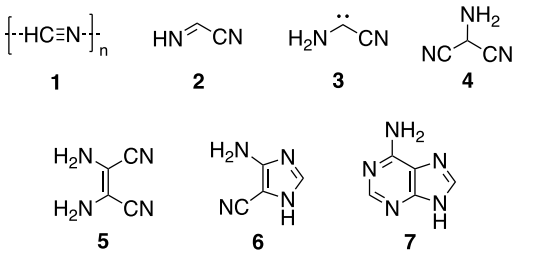

Figure 1. Different molecules linked to HCN-derived polymers.

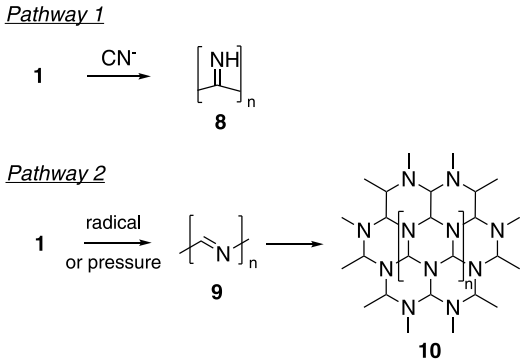

Figure 2. Examples of HCN polymerization pathways catalyzed in different ways. Top: base-catalyzed formation of polyimine (**8**).[15] Bottom: radical-catalyzed[31,32,35] and/or pressure-induced[35] formation of one- and two-dimensional materials.

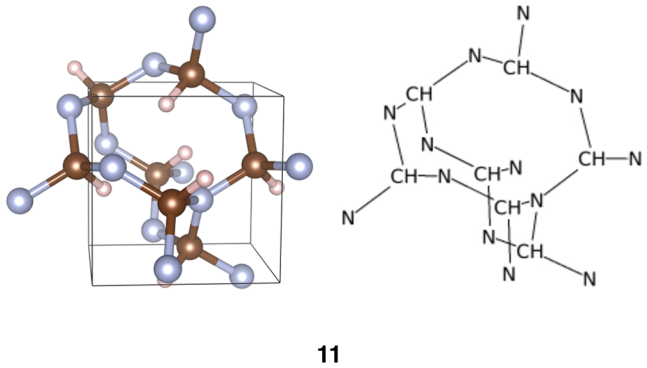

Figure 3. Three-dimensional HCN-derived polymer (**11**).[36] Left: color representations: carbon—brown, hydrogen—pink, and nitrogen—gray.

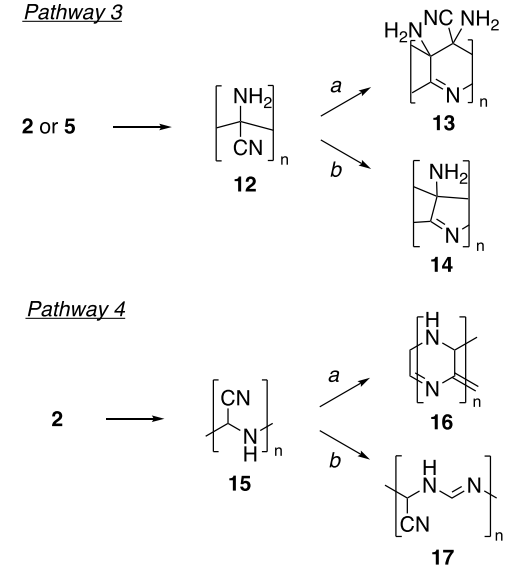

Figure 4. Products of iminoacetonitrile (**2**) polymerization proposed by Völker[13] and Umemoto[33] (pathways 3a and 3b), and Ruiz-Bermejo and colleagues[11] (pathways 4a and 4b).

https://doi.org/10.1021/acsearthspacechem.4c00088
ACS Earth Space Chem. 2024, 8, 1272−1280

readily produced in polymerization experiments.[16,31,34] One suggested role of **5** is as an intermediate in the hypothesized formation of **7**.[25,34] The structure **5** is known to undergo photochemical isomerization to **6**.[8,38] It has been suggested[15,17,39] that the *cis*- and *trans*-forms of **5** are possible starting points for the Völker[13] and Umemoto[33] models (**12**, **13**, and **14**) shown in Figure 4.[15,30] Other structures proposed to form from **5** include the linear polymers **21** and **22** (Figure 5, pathway 6).[11]

Polyaminomalononitrile (23). Figure 6 shows the two last pathways that we consider. Interest in polyaminomalononitrile (**23**) is motivated by a suggestion by Matthews and Moser: that **23** may be a precursor to polypeptides.[29] This proposal has been criticized for lack of experimental evidence.[40,41] **3**, **4**, and **5** have been proposed as precursors to **23** (Figure 6, pathways 7 and 8).[11,27−29,42]

To facilitate comparison with laboratory experiments, predicted thermodynamics of reaction (ΔG^{o}_{298K}) are provided under standard conditions of temperature (298 K) and concentration (1 M). Relevant experiments have been conducted in a wide range of temperatures: HCN (195−363 K),[16] **2** (>233 K),[43] **4** (∼298 K),[18,44] and **5** (298−483 K).[16,24] We note that astrochemical environments rich in HCN, such as Saturn's moon Titan, can be considerably colder than the temperature of our estimates and in most experiments. Although the main conclusions drawn from our predictions are largely unaffected by changes in temperature, there are some exceptions that we will return to discuss. Estimating the temperature dependence of thermodynamic stability for our entire collection of materials is beyond the scope of this work.

RESULTS AND DISCUSSION

In this work, we compute the free energy of all of the above-mentioned structures as well as a few additional ones. Our study makes use of a sampling algorithm to identify candidates to the lowest-energy ground states in the vast configurational space of the HCN-derived molecules and polymers (see the Methods section for details).[45] To limit computational costs, polymers have been represented as oligomers of approximately 60 atoms. Figure 7 exemplifies predicted stable conformers for three such structures evaluated with the implicit consideration of water solvation. Most experimental literature studies have been performed in aqueous solution (see ref 11 for a review) or in neat liquid HCN.[15,31,32] HCN and water are both polar and hydrogen bonding solvents and can be expected to cause comparable trends in the relative solvation energies.

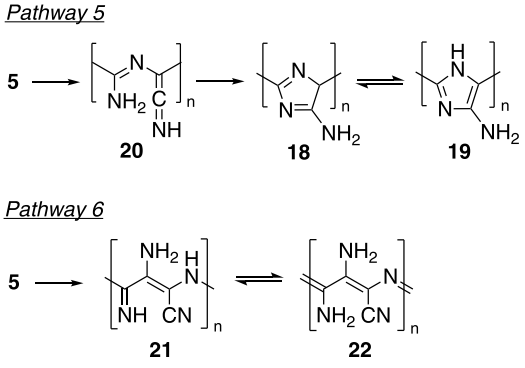

Figure 5. Two pathways for polymerization of diaminomaleonitrile (**5**) proposed in the literature.[11,31]

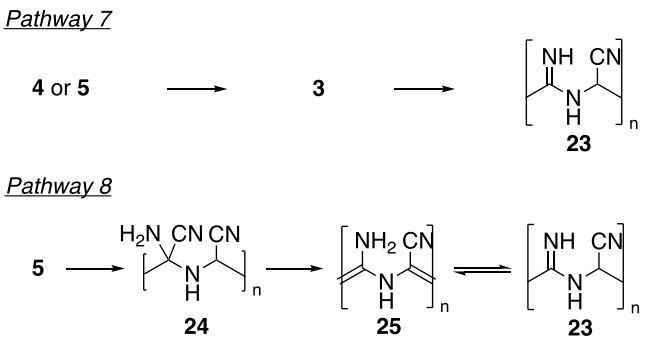

Figure 6. Proposed pathways to form polyaminomalononitrile (**23**).[11,27−29,42]

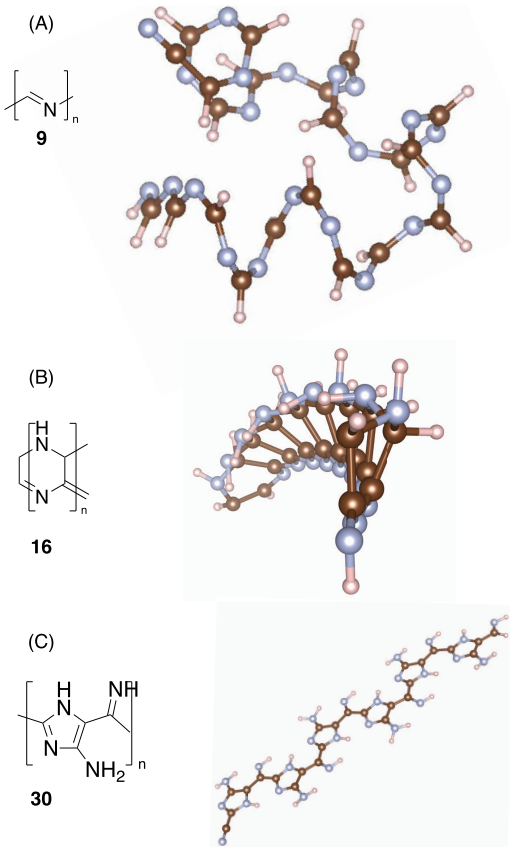

Figure 7. Examples of predicted HCN oligomer structures. (A) Head-to-tail polymer (**9**), (B) cyclic polymer (**16**), (C) copolymer (**26**) of repeating units belonging to **19** and **8**. Color representations: carbon—brown, hydrogen—pink, and nitrogen—gray.

Figure 8 summarizes our best estimates for the relative Gibbs free energy of all considered structures. Corresponding relative energies in the absence of solvation are available in the Supporting Information.

The energy content per HCN in the studied structures varies between +7.5 and −16.1 kcal/mol (Figure 8). In other words, note that to arrive at a reaction energy, the values shown in Figure 8 need to be multiplied with the number of HCN in each structure. For example, for adenine, this multiplication factor is 5, while for a polymer, it is *n*. Most investigated structures are clearly thermodynamically downhill from HCN in aqueous solution at 298 K. The overall thermodynamic favorability of HCN self-reactions is thus one part of the explanation for the commonly observed chemical complexity

https://doi.org/10.1021/acsearthspacechem.4c00088
ACS Earth Space Chem. 2024, 8, 1272−1280

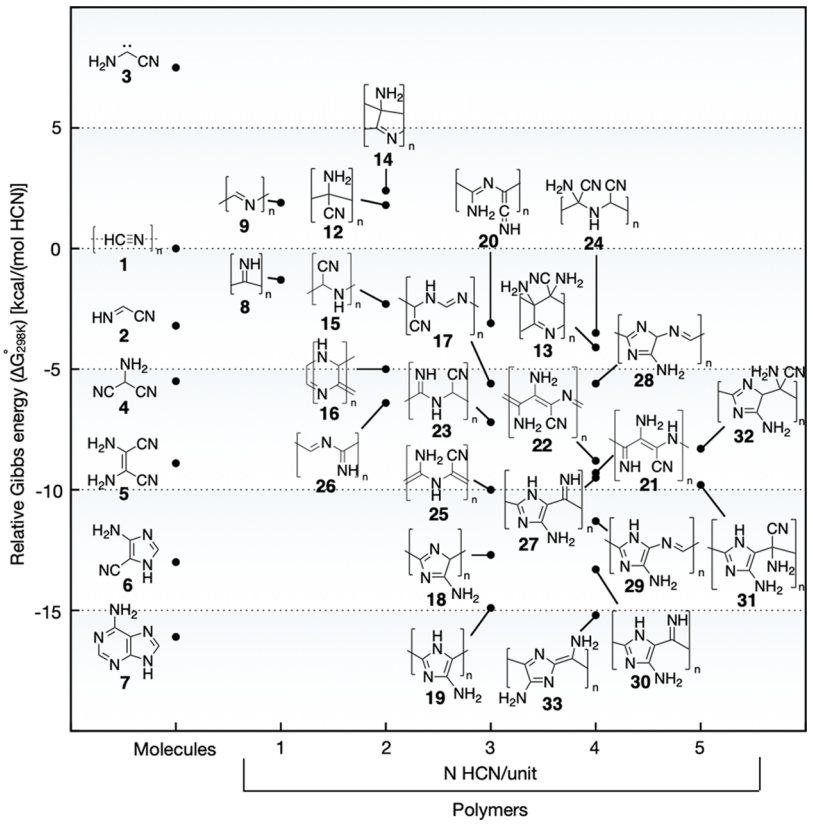

Figure 8. Thermodynamic landscape of HCN-derived structures. Gibbs energies (ΔG^{o}_{298K}) are provided per mole of HCN and relative to a reference chain of HCN molecules. Polymeric materials are organized by the number of HCN molecules in their monomer unit.

of reaction mixtures. The only materials predicted to be unstable relative to HCN are **3**, **9**, **12**, and **14**, effectively ruling these out as plausible reaction products under the studied conditions.

Our calculations infer new insight into the viability of Völker's suggestion that **2** is the monomer unit of **12** and **13** (Figure 4, pathway 3a). Our data predict that the formation of **13** from **2** is thermodynamically favored. At the same time, we can rule out **12** as a major product since it is unstable relative to **2**, as well as **8** + **1** (and most other structures). We can also rule out Umemoto's single-ladder model (**14**) (Figure 4, pathway 3b) as a plausible polymerization product on the grounds of unfavorable thermodynamics.

Figure 8 shows that **5** is more stable than most of the considered structures. This prediction has several important consequences. For example, structures **12**, **13**, and **14** are unlikely to be the products of polymerization of **5** because such transformations are predicted to be thermodynamically unfavored. Other similar examples include structures **23** and **20**, predicted to lie ∼1.7 and 5.8 kcal/mol of HCN above **5**, respectively. Establishing that the formation of **23** from **5** is not thermodynamically spontaneous is important as the former is a proposed precursor to heteropolypeptides.[27,40] However, we note that our predictions do not exclude the possibility of **23** forming through other higher-energy intermediates, such as the HCN trimer **4** ($\Delta G^{o}_{298\,K}$ = −1.7 kcal/mol HCN).

We have found only a limited number of HCN-derived polymers and molecules to be thermodynamically downhill relative to **5**. For example, and in agreement with previous theoretical studies,[46] the formation of **7** from **5** is thermodynamically allowed. The linear polymer **21** is another example that could feasibly form from **5**. Structures **19** and **33** are predicted to be the most stable polymers out of those considered, with only molecule **7** being more stable. Formation of **19** and **33** from **5** is predicted to be spontaneous by −6.0 and −6.3 kcal/mol of HCN, respectively. The corresponding polymerization enthalpy ($\Delta H^{o}_{298\,K}$) is calculated as −9.9 and −9.7 kcal/mol of HCN (Supporting Information, Table S3). These energies are in fair agreement with estimates derived from differential scanning calorimetry thermograms of solid state and melt polymerization of **5**.[17] That study, by Ruiz-Bermejo and colleagues, estimated heat releases of 3−5 kcal/mol HCN at 423−463 K.[17]

We furthermore predict that the HCN dimer **3** has an energy content of +7.5 kcal/mol HCN, i.e., its formation from HCN is uphill by 15 kcal/mol. This value is 8.4 kcal/mol lower than the corresponding value in gas phase (Supporting Information, Table S1), in turn comparable to other computational results.[43,47] We note that **3** has a similar energy content to hydrogen isocyanide in solution.[48] Nevertheless, **3** is high in energy and can be ruled out as a major component of reaction mixtures.

Energy of Two- and Three-Dimensional Materials. Our methodology used for calculating the data shown in Figure 8 is limited to molecules and one-dimensional polymers. For polymers with higher-dimensional connectivity, we have relied on DFT calculations with periodic boundary conditions (see the Methods section). Figure 9 shows our stability estimates for 2D and 3D polymers **10** and **11**. Both systems are composed of tetrahedrally coordinated C and N atoms in a graphane-like configuration (Figure 9). Phonon band structures of **10** (including the isomers **10A** and **10B**)

https://doi.org/10.1021/acsearthspacechem.4c00088
ACS Earth Space Chem. 2024, 8, 1272−1280

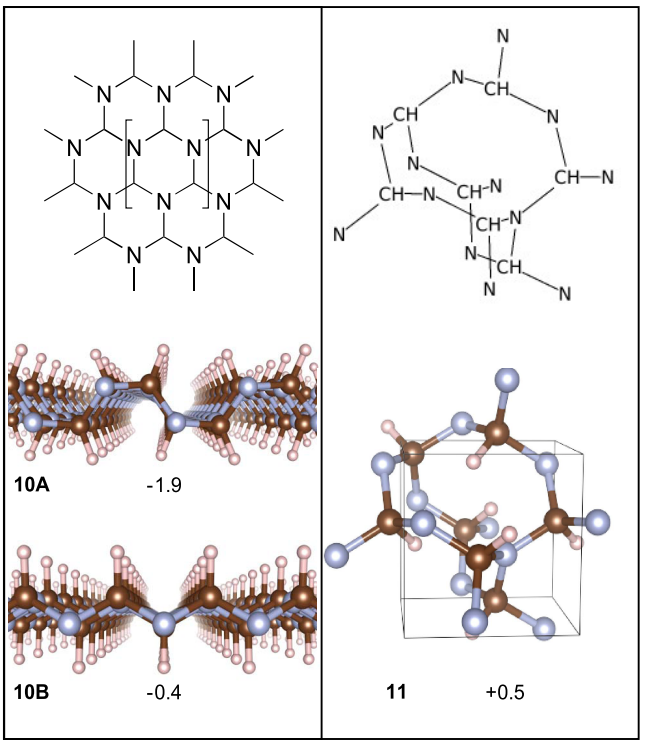

Figure 9. Structure and predicted energies of **10** and **11**. Gibbs energies ($\Delta G_{298\,K}{}^{0}$) in kcal/mol are provided relative to an infinite chain of HCN molecules in vacuum. Color representations: carbon—brown, hydrogen—pink, and nitrogen—gray.

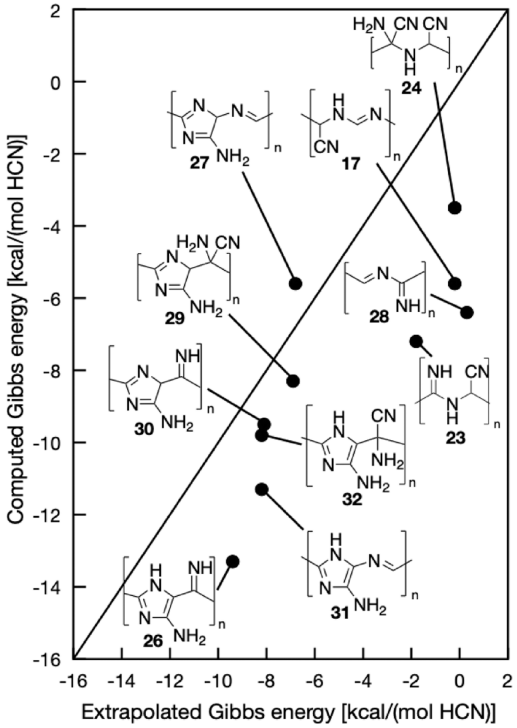

Figure 10. Quantum mechanically calculated stability (c.f. Figure 8) plotted against a weighted average extrapolation of known energies of smaller subunits (see the Methods section). The mean absolute error is 3.3 kcal/mol.

and **11**, provided in the Supporting Information (Figures S2–S4), confirm that these materials are dynamically stable. In other words, these structures all constitute local minima on the potential energy surface, which allows us to account for temperature effects in our relative stability estimates. Although structures **10A** and **10B** are calculated as only slightly thermodynamically favored (−1.9- − 0.4) relative to our reference of an infinite chain of HCN molecules at ambient conditions (Figure S1), **11** is instead predicted to be unstable by +0.5 kcal/mol.

Approximate Stability Prediction of HCN-Based Polymers. The repeating units of several structures in Figure 8 can be considered combinations of simpler monomer units. For example, structure **23** can be viewed as a combination of **8** and **15** (Figure 8). Figure 10 illustrates how our calculated energies of smaller polymer units can be used to estimate the relative energies of more complex HCN-based structures through a weighted averaging approach (see the Methods section for details). Such linear extrapolation is approximate and can be expected to fail, e.g., in the presence of extensive conjugation. Nonetheless, this approach constitutes a rapid route to exploring the thermodynamics of a larger structural space of HCN-derived materials.

Effect of Temperature. Before speculating on the consequences of our predictions on different astrochemical environments, we remind that relative Gibbs energies depend on temperature. To understand such dependencies, we recall that the Gibbs energy can be expressed as

$$\Delta G = \Delta H - T\Delta S \quad (1)$$

where H is the enthalpy, T is the temperature, and S is the entropy. The energies we discuss (Figures 8 and 9) include corrections for enthalpic and entropic contributions at 298 K. This choice was made to approximately align with experiments, typically performed under near Earth ambient conditions. Although the broad strokes of the presented thermodynamic map will persist at lower temperatures, changes in the order of a few kcal/mol can be expected. In general, relative enthalpies (ΔH) are not substantially affected by temperature and Tables S1–S4 exemplify how $\Delta H_{298\,K}$ is approximately equal to $\Delta H_{T\to 0\,K}$ (ΔE including zero-point energy) for a selection of studied reactions.

The largest temperature effect on our Gibbs energy estimates derives from changing entropy, the $T\Delta S$-term of eq 1. The combination of HCN molecules with progressively larger structures is resisted by decreasing entropy ($\Delta S < 0$), a change dominated by the removal of rotational and translational degrees of freedom. In low-temperature environments, such as those on Titan, the resulting entropic penalty for making larger molecules and polymers ($-T\Delta S$) decreases. Figure 11 exemplifies how such entropy-driven temperature effects can disfavor the formation of smaller molecules, relative to polymerization. In other words, thermodynamic changes brought by temperatures dropping, e.g., from Earth to Titan surface conditions, can change the outcome of prebiotic reaction chemistry.

CONCLUSIONS

Our study shows that several hypotheses regarding HCN's reactions to molecules and polymers can be ruled out on the grounds of thermodynamics. For example, diaminomaleonitrile (**5**), a prominently suggested reaction intermediate in HCN-based prebiotic chemistry, is predicted to be lower in energy compared with many proposed polymer products. Our study also infers a new perspective on adenine (**7**), a nucleobase,

https://doi.org/10.1021/acsearthspacechem.4c00088
ACS Earth Space Chem. 2024, 8, 1272−1280

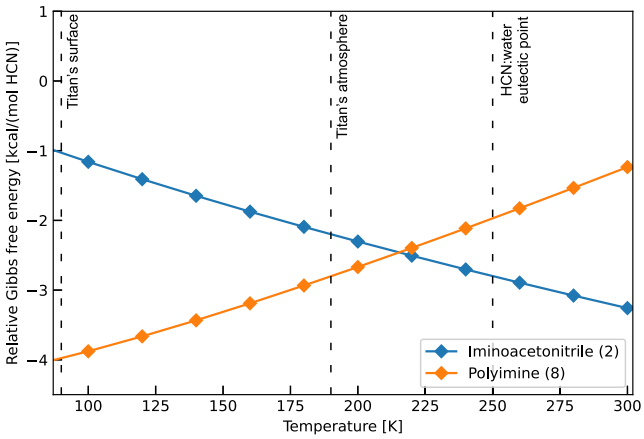

Figure 11. Example of how temperature can affect the relative stability of HCN-derived materials. As the temperature drops below the eutectic point of HCN:water mixtures, polyimine (**8**) becomes favored over the HCN dimer iminoacetonitrile (**2**). Such stability inversions may have consequences for chemical evolution in cold environments, e.g., in the atmosphere and surface of Saturn's moon Titan.

present in all life as we currently know it (Figure 8). Formation of **7** is predicted to be thermodynamically downhill from *all* structures considered herein under ambient conditions. The low experimental yields (<0.01%[8]) of **7** from HCN in typical condensed phase experiments therefore means such reactions must be kinetically controlled. One class of materials that closely competes with the thermodynamic favorability of adenine is polyaminoimidazoles (**19**, Figure 5, pathway 5). In other words, under the assumption that reaction kinetics are permissive, structures such as **19** and **33** should be expected as products of HCN self-reaction chemistry.

The presented thermodynamic landscape of HCN-derived materials has several consequences for interpreting HCN's reactivity in various astrochemical environments, in and beyond the solar system. Most (but not all) previously proposed HCN-derived polymers and molecules can form spontaneously ($\Delta G_r < 0$) close to Earth ambient conditions. In low-temperature environments, such as those on Titan, the entropic penalty for making larger molecules and polymers ($-T\Delta S$) naturally decreases. In other words, the chances for thermodynamic spontaneity of macromolecular formation increase in cold environments.

We end by emphasizing that thermodynamics is only one side of the chemical reactivity coin. At the same time, as more structures can become thermodynamically viable at lower temperatures, such chemistry will naturally be more limited by reaction kinetics.[49] Enhanced kinetic control of HCN-based prebiotic chemistry means a greater ability of colder environments to generate specific metastable products from an increased pool of thermodynamically allowed options. We can therefore speculate on the potential of colder worlds, such as Titan, in generating kinetically selected products that may otherwise not form at higher temperatures. Some such materials could, hypothetically, be crucial templates for the origin of life.[10] We report on reaction kinetics for the formation of **2**, **4**, **5**, and **8** in refs 49 and 50, and will return in future work with a detailed study of the formation of adenine (**7**).

METHODS

Conformational Search. The Conformer-Rotamer Ensemble Sampling Tool (CREST)[45] was used in automated searches of lowest-lying conformers of molecules and oligomers. The energy evaluations in CREST make use of the semiempirical xtb program, version 6.4.0.[51] Conformational structure searches in aqueous solution were performed with the analytical linearized Poisson−Boltzmann (ALPB) model.[52] Structural differences between predicted larger and smaller oligomers risk influencing the computed energy content, e.g., through different end-effects. We therefore additionally relied on visual inspection to ensure models of oligomers of different lengths were similar in appearance/folding.

Electronic Structure Calculations. With the exception for two and three-dimensional networks, all structures were optimized using the B3LYP[53] functional, as implemented in Gaussian 16, revision B.01.[54] Missing treatment of dispersion effects in B3LYP was corrected for using Grimme's method combined with Becke-Johnson damping (D3BJ).[55] The standard polarizable continuum (PCM) model of Gaussian was used to model interactions with water solvent.[56] Our best estimate to total Gibbs free energies, G_f, was calculated as

$$G_f = E_f + G_{corr} \quad (2)$$

where G_{corr} denotes thermal corrections obtained following optimization and frequency analyses using the cc-pVDZ basis set. Final electronic energies, E_f, in eq 2 were calculated as single-point calculations at the B3LYP-D3BJ/aug-cc-pVTZ level of theory. Method validations were performed against the M06-2X[57] meta-GGA functional, and close agreement was found (Tables S2 and S4). The average absolute deviation between B3LYP-D3 and M06-2X results in PCM-water is 0.65 kcal/mol, with a maximum of 3.2 kcal/mol for compound **9**.

Calculations of Extended Structures. Periodic DFT calculations were carried out using the Vienna Ab Initio Simulation Package (VASP)[58] version 5.4.4. The B3LYP-D3BJ level of theory was used for both structure optimizations and calculations of phonon spectra. These calculations relied on projected augmented wave (PAW) potentials[59] used together with a plane wave kinetic energy cutoff of 800 eV. Γ-Centered *k*-point mesh with a resolution < 2π 0.066 Å^{-1} was used for integration over reciprocal space. Two-dimensional polymers were separated by 30 Å vacuum layers. Energies and forces were converged to less than 1 meV/atom and 1 meV/(Å × atom), respectively. Thermal corrections were calculated using PHONOPY[60] version 2.11.0 using supercell dimensions of 2 × 2 × 2, 2 × 2 × 1, and 4 × 1 × 2 for the **11**, **10A**, and **10B** polymers, respectively.

Estimating the Stability of Molecules. The average energy per unit of HCN is here used when comparing different materials

$$\Delta G^0_{298\,K} = \frac{G_{molecule}}{k} - G_{HCN} \quad (3)$$

where $G_{molecule}$ is the total free energy of the molecule, k is the number of HCN in the molecule, and G_{HCN} is the average energy of HCN inside a one-dimensional H-bonded chain.

Estimating the Stability of Polymers. The average Gibbs energy per unit of HCN inside polymeric materials is here evaluated as

https://doi.org/10.1021/acsearthspacechem.4c00088
ACS Earth Space Chem. 2024, 8, 1272−1280

$$\Delta G^{0}_{298\ \mathrm{K}} = \frac{G_{\mathrm{f,Long}} - G_{\mathrm{f,Short}}}{k} - G_{\mathrm{HCN}} \quad (4)$$

where $G_{\mathrm{f,Long}}$ and $G_{\mathrm{f,Short}}$ are the total free energies of the (n)-long and (n-k)-short polymer models, respectively, n is the number of HCN in the long oligomer model, and k is the number of HCN in a monomer unit. The sizes of our oligomer models were chosen to have at least 4 repeating polymer units, and n is always near 20. Each polymer model was capped by a cyanide group at one end and a hydrogen atom at the other end.

Computing the Energies of 10 and 11. Thermodynamic stabilities of **10A**, **10B**, and **11** were estimated by dividing the calculated total energy of each material by the number of HCN in its unit cell, and by subtracting the average energy of HCN in an infinite hydrogen-bonded chain. Our molecular and periodic calculations are of comparable levels of theory, also evidenced by the hydrogen bond distances between HCN differing by less than 0.025 Å.

Energy Estimates of Composite Polymers. The Gibbs free energy content of HCN in composite polymers, G_{cp}, can, as a first approximation, be estimated from a weighted average of our quantum mechanically computed free energies $G_{\mathrm{f},i}$,

$$G_{\mathrm{cp}} = \frac{\sum_{i=1}^{l} k_i G_{\mathrm{f},i}}{\sum_{i=1}^{l} k_i} \quad (5)$$

where k_i is the number of HCN in the polymer units of polymers i and l is the number of monomer units in the combined polymer.

■ ASSOCIATED CONTENT

Supporting Information

The Supporting Information is available free of charge at https://pubs.acs.org/doi/10.1021/acsearthspacechem.4c00088.

Relative free energy, enthalpy, and zero-point energies in aqueous solution; relative free energy, enthalpy and zero-point energies in vacuum; and phonon bands of structures **10A**, **10B**, and **11** (PDF)

■ AUTHOR INFORMATION

Corresponding Author

Martin Rahm − *Department of Chemistry and Chemical Engineering, Chalmers University of Technology, Gothenburg 412 96, Sweden;* orcid.org/0000-0001-7645-5923; Email: martin.rahm@chalmers.se

Authors

Hilda Sandström − *Department of Chemistry and Chemical Engineering, Chalmers University of Technology, Gothenburg 412 96, Sweden;* Present Address: Department of Applied Physics, Aalto University, P.O. Box 11100, 00076 Espoo, Finland

Fernando Izquierdo-Ruiz − *Department of Chemistry and Chemical Engineering, Chalmers University of Technology, Gothenburg 412 96, Sweden;* Present Address: Department of Physical Chemistry, Complutense University of Madrid, Plaza de las ciencias 2, 28040 Madrid, Spain; orcid.org/0000-0001-7237-4720

Marco Cappelletti − *Department of Chemistry and Chemical Engineering, Chalmers University of Technology, Gothenburg 412 96, Sweden*

Rana Dogan − *Department of Chemistry and Chemical Engineering, Chalmers University of Technology, Gothenburg 412 96, Sweden*

Siddhant Sharma − *Department of Chemistry and Chemical Engineering, Chalmers University of Technology, Gothenburg 412 96, Sweden;* Present Address: Department of Biology, Ashoka University, Sonipat, 131029 Haryana, India.

Clara Bailey − *Department of Chemistry and Chemical Engineering, Chalmers University of Technology, Gothenburg 412 96, Sweden*

Complete contact information is available at: https://pubs.acs.org/10.1021/acsearthspacechem.4c00088

Author Contributions

Conceptualization: M.R. Investigation: H.S., F.I.-R., M.C., R.D., S.S., C.B. Methodology: H.S., M.R., F.I.-R. Writing—original draft: H.S., M.R., F.I.-R.

Funding

The authors acknowledge funding from the Swedish Research Council (grants 2016-04127 and 2020-04305) and Chalmers University of Technology. Their research relied on computational resources provided by the Swedish National Infrastructure for Computing (SNIC) at C3SE, NSC, and PDC partially funded by the Swedish Research Council through grant agreement no. 2018-05973 and by the National Academic Infrastructure for Supercomputing in Sweden (NAISS) at C3SE and NSC partially funded by the Swedish research council through grant agreement no. 2022-06725. F.I.-R. acknowledges the Government of Principado de Asturias for its support through FICYT grant number AYUD/2021/58773. S.S. acknowledges support and funding from the Chalmers Astrophysics and Space Sciences Summer (CASSUM) research fellowship.

Notes

The authors declare no competing financial interest.

■ ABBREVIATIONS

HCN, hydrogen cyanide; DFT, density functional theory; CREST, Conformer-Rotamer Ensemble Sampling Tool; ALPB, analytical linearized Poisson−Boltzmann; VASP, Vienna Ab initio Simulation Package; PAW, projected augmented wave; B3LYP, Becke, 3-parameter, Lee−Yang−Parr

■ REFERENCES

(1) (a) Tokunaga, A. T.; Beck, S. C.; Geballe, T. R.; Lacy, J. H.; Serabyn, E. The detection of HCN on Jupiter. *Icarus* **1981**, *48*, 283−289. (b) Lellouch, E.; Romani, P. N.; Rosenqvist, J. The vertical Distribution and Origin of HCN in Neptune's Atmosphere. *Icarus* **1994**, *108*, 112−136.

(2) Lellouch, E.; Gurwell, M.; Butler, B.; Fouchet, T.; Lavvas, P.; Strobel, D. F.; Sicardy, B.; Moullet, A.; Moreno, R.; Bockelée-Morvan, D.; Biver, N.; Young, L.; Lis, D.; Stansberry, J.; Stern, A.; Weaver, H.; Young, E.; Zhu, X.; Boissier, J. Detection of CO and HCN in Pluto's atmosphere with ALMA. *Icarus* **2017**, *286*, 289−307.

(3) Tanguy, L.; Bézard, B.; Marten, A.; Gautier, D.; Gérard, E.; Paubert, G.; Lecacheux, A. Stratospheric profile of HCN on Titan from millimeter observations. *Icarus* **1990**, *85*, 43−57.

(4) Rodgers, S. D.; Charnley, S. B. HNC and HCN in Comets. *Astrophys J. Lett.* **1998**, *501*, L227.

(5) Buhl, D.; Snyder, L. E. Unidentified Interstellar Microwave Line. *Nature* **1970**, *228*, 267.

(6) (a) Rimmer, P. B.; Shorttle, O. A Surface Hydrothermal Source of Nitriles and Isonitriles. *Life* **2024**, *14*, 498. (b) Ferus, M.; Kubelík, P.; Knížek, A.; Pastorek, A.; Sutherland, J.; Civiš, S. High Energy

Radical Chemistry Formation of HCN-rich Atmospheres on early Earth. *Sci. Rep.* **2017**, *7*, No. 6275. (c) Airapetian, V. S.; Glocer, A.; Gronoff, G.; Hébrard, E.; Danchi, W. Prebiotic chemistry and atmospheric warming of early Earth by an active young Sun. *Nat. Geosci.* **2016**, *9*, 452−455. (d) Tian, F.; Kasting, J. F.; Zahnle, K. Revisiting HCN formation in Earth's early atmosphere. *Earth Planet. Sci. Lett.* **2011**, *308*, 417−423.

(7) Marín-Yaseli, M. R.; Mompeán, C.; Ruiz-Bermejo, M. A Prebiotic Synthesis of Pterins. *Chem.—Eur. J.* **2015**, *21*, 13531−13534.

(8) Ruiz-Bermejo, M.; Zorzano, M.-P.; Osuna-Esteban, S. Simple organics and biomonomers identified in HCN polymers: an overview. *Life* **2013**, *3*, 421−448.

(9) (a) Perrin, Z.; Carrasco, N.; Chatain, A.; Jovanovic, L.; Vettier, L.; Ruscassier, N.; Cernogora, G. An Atmospheric Origin for HCN-Derived Polymers on Titan. *Processes* **2021**, *9*, 965. (b) Matthews, C. N.; Ludicky, R. Hydrogen cyanide polymers on comets. *Adv. Space Res.* **1992**, *12*, 21−32. (c) Lis, D. C.; Bockelée-Morvan, D.; Boissier, J.; Crovisier, J.; Biver, N.; Charnley, S. B. Hydrogen Isocyanide in Comet 73P/Schwassmann-Wachmann (Fragment B). *Astrophys. J.* **2008**, *675*, 931−936.

(10) Rahm, M.; Lunine, J. I.; Usher, D.; Shalloway, D. Polymorphism and electronic structure of polyimine and its potential significance for prebiotic chemistry on Titan. *Proc. Natl. Acad. Sci. U.S.A.* **2016**, *113*, 8121−8126.

(11) Ruiz-Bermejo, M.; de la Fuente, J. L.; Pérez-Fernández, C.; Mateo-Martí, E. A Comprehensive Review of HCN-Derived Polymers. *Processes* **2021**, *9*, 597.

(12) Marin-Yaseli, M. R.; Moreno, M.; de la Fuente, J. L.; Briones, C.; Ruiz-Bermejo, M. Experimental conditions affecting the kinetics of aqueous HCN polymerization as revealed by UV−vis spectroscopy. *Spectrochim Acta A Mol. Biomol. Spectrosc.* **2018**, *191*, 389−397.

(13) Völker, T. Polymere Blausäure. *Angew. Chem.* **1960**, *72*, 379−384.

(14) (a) Mas, I.; de la Fuente, J. L.; Ruiz-Bermejo, M. Temperature effect on aqueous NH4CN polymerization: Relationship between kinetic behaviour and structural properties. *Eur. Polym. J.* **2020**, *132*, No. 109719. (b) Bonnet, J.-Y.; Thissen, R.; Frisari, M.; Vuitton, V.; Quirico, E.; Orthous-Daunay, F.-R.; Dutuit, O.; Roy, L. L.; Fray, N.; Cottin, H.; Horst, S. M.; Yelle, R. V. Compositional and structural investigation of HCN polymer through high resolution mass spectrometry. *Int. J. Mass Spectrom.* **2013**, *354*−*355*, 193−203. (c) Garbow, J. R.; Schaefer, J.; Ludicky, R.; Matthews, C. N. Detection of secondary amides in hydrogen cyanide polymers by dipolar rotational spin-echo nitrogen-15 NMR. *Macromolecules* **1987**, *20*, 305−309. (d) Ruiz-Bermejo, M.; de la Fuente, J. L.; Rogero, C.; Menor-Salvan, C.; Osuna-Esteban, S.; Martin-Gago, J. A. New Insights into the Characterization of 'Insoluble Black HCN Polymers'. *Chem. Biodiversity* **2012**, *9*, 25−40.

(15) He, C.; Lin, G.; Upton, K. T.; Imanaka, H.; Smith, M. A. Structural Investigation of HCN Polymer Isotopomers by Solution-State Multidimensional NMR. *J. Phys. Chem. A* **2012**, *116*, 4751−4759.

(16) Ruiz-Bermejo, M.; de la Fuente, J. L.; Carretero-Gonzalez, J.; Garcia-Fernandez, L.; Aguilar, M. R. A Comparative Study on HCN Polymers Synthesized by Polymerization of NH4 CN or Diaminomaleonitrile in Aqueous Media: New Perspectives for Prebiotic Chemistry and Materials Science. *Chem.—Eur. J.* **2019**, *25*, 11437−11455.

(17) Ruiz-Bermejo, M.; García-Armada, P.; Mateo-Martí, E.; de la Fuente, J. L. HCN-derived polymers from thermally induced polymerization of diaminomaleonitrile: A non-enzymatic peroxide sensor based on prebiotic chemistry. *Eur. Polym. J.* **2022**, *162*, No. 110897.

(18) Thissen, H.; Koegler, A.; Salwiczek, M.; Easton, C. D.; Qu, Y.; Lithgow, T.; Evans, R. A. Prebiotic-chemistry inspired polymer coatings for biomedical and material science applications. *NPG Asia Mater.* **2015**, *7*, No. e225.

(19) Asha, A. B.; Ounkaew, A.; Peng, Y.-Y.; Gholipour, M. R.; Ishihara, K.; Liu, Y.; Narain, R. Bioinspired antifouling and antibacterial polymer coating with intrinsic self-healing property. *Biomater. Sci.* **2022**, *11*, 128−139.

(20) Nandi, S.; Bhattacharyya, D.; Anoop, A. Prebiotic Chemistry of HCN Tetramerization by Automated Reaction Search. *Chem.—Eur. J.* **2018**, *24*, 4885−4894.

(21) Zhang, H.; Wang, J.; Guégan, F.; Frapper, G. First-principles structure prediction of two-dimensional HCN polymorphs obtained via formal molecular polymerization. *Nanoscale* **2023**, *15*, 7472−7481.

(22) Panda, S.; Anoop, A. Potential Prebiotic Pathways in Extraterrestrial Atmosphere: A Computational Exploration of HCN and NH_3 Reactions. *ACS Earth Space Chem.* **2024**, *8*, 348−360.

(23) Hortelano, C.; Ruiz-Bermejo, M.; de la Fuente, J. L. Solid-state polymerization of diaminomaleonitrile: Toward a new generation of conjugated functional materials. *Polymer* **2021**, *223*, No. 123696.

(24) Mas, I.; Hortelano, C.; Ruiz-Bermejo, M.; de la Fuente, J. L. Highly efficient melt polymerization of diaminomaleonitrile. *Eur. Polym. J.* **2021**, *143*, No. 110185.

(25) Oro, J. Mechanism of synthesis of adenine from HCN under possible primitive earth conditions. *Nature* **1961**, *191*, 1193−1194.

(26) Sanchez, R. A.; Ferris, J. P.; Orgel, L. E. Prebiotic synthesis. II. Synthesis of purine precursors and amino acids from aqueous hydrogen cyanide. *J. Mol. Biol.* **1967**, *30*, 223−253.

(27) Moser, R. E.; Claggett, A. R.; Matthews, C. N. Peptide formation from diaminomaleonitrile (HCN tetramer). *Tetrahedron Lett.* **1968**, *9*, 1599−1603.

(28) Moser, R. E.; Claggett, A. R.; Matthews, C. N. Peptide formation from aminomalononitrile (HCN trimer). *Tetrahedron Lett.* **1968**, *9*, 1605−1608.

(29) Matthews, C. N.; Moser, R. E. Prebiological protein synthesis. *Proc. Natl. Acad. Sci. U. S. A.* **1966**, *56*, 1087−1094.

(30) Mamajanov, I.; Herzfeld, J. HCN polymers characterized by SSNMR: Solid state reaction of crystalline tetramer (diaminomaleonitrile). *J. Chem. Phys.* **2009**, *130*, 134504/1−134504/5.

(31) Mamajanov, I.; Herzfeld, J. HCN polymers characterized by solid state NMR: Chains and sheets formed in the neat liquid. *J. Chem. Phys.* **2009**, *130*, 134503/1−134503/6.

(32) Mozhaev, P. S.; Kichigina, G. A.; Kiryukhin, D. P.; Barkalov, I. M. Radiation-induced polymerization of hydrogen cyanide. *High Energy Chem. (Transl. of Khim. Vys. Energy)* **1995**, *29*, 15−18.

(33) Umemoto, K.; Takahasi, M.; Yokota, K. Studies on the structure of HCN oligomers. *Origins of life and evolution of the biosphere* **1987**, *17*, 283−293.

(34) Sanchez, R.; Ferris, J.; Orgel, L. E. Conditions for Purine Synthesis: Did Prebiotic Synthesis Occur at Low Temperatures. *Science* **1966**, *153*, 72.

(35) Khazaei, M.; Liang, Y.; Bahramy, M. S.; Pichierri, F.; Esfarjani, K.; Kawazoe, Y. High-pressure phases of hydrogen cyanide: formation of hydrogenated carbon nitride polymers and layers and their electronic properties. *J. Phys.: Condens. Matter* **2011**, *23*, 405403/1−405403/12.

(36) Eremets, M. I.; Gavriliuk, A. G.; Trojan, I. A.; Dzivenko, D. A.; Boehler, R. Single-bonded cubic form of nitrogen. *Nat. Mater.* **2004**, *3*, 558−563.

(37) Lian, C.-S.; Wang, X.-Q.; Wang, J.-T. Hydrogenated K4 carbon: A new stable cubic gauche structure of carbon hydride. *J. Chem. Phys.* **2013**, *138*, 024702/1−024702/5.

(38) (a) Ferris, J. P.; Orgel, L. E. Aminomalononitrile and 4-amino-5-cyanoimidazole in hydrogen cyanide polymerization and adenine synthesis. *J. Am. Chem. Soc.* **1965**, *87*, 4976−4977. (b) Boulanger, E.; Anoop, A.; Nachtigallova, D.; Thiel, W.; Barbatti, M. Photochemical Steps in the Prebiotic Synthesis of Purine Precursors from HCN. *Angew. Chem., Int. Ed.* **2013**, *52*, 8000−8003.

(39) Matthews, C. N.; Minard, R. D. Hydrogen cyanide polymers, comets and the origin of life. *Faraday Discuss.* **2006**, *133*, 393−401.

(40) Ferris, J. P. Hydrogen cyanide did not condense to give heteropolypeptides on the primitive Earth. *Science* **1979**, *203*, 1135−1136.

https://doi.org/10.1021/acsearthspacechem.4c00088
ACS Earth Space Chem. 2024, 8, 1272−1280

(41) (a) Ferris, J. P.; Edelson, E. H.; Auyeung, J. M.; Joshi, P. C. Structural studies on HCN oligomers. *J. Mol. Evol* **1981**, *17*, 69−77. (b) Ferris, J. P.; Donner, D. B.; Lotz, W. Chemical evolution. IX. Mechanism of the oligomerization of hydrogen cyanide and its possible role in the origins of life. *J. Am. Chem. Soc.* **1972**, *94*, 6968−6974.
(42) Matthews, C.; Nelson, J.; Varma, P.; Minard, R. Deuterolysis of amino acid precursors: evidence for hydrogen cyanide polymers as protein ancestors. *Science* **1977**, *198*, 622.
(43) Evans, R. A.; Lorencak, P.; Ha, T. K.; Wentrup, C. HCN dimers: iminoacetonitrile and N-cyanomethanimine. *J. Am. Chem. Soc.* **1991**, *113*, 7261−7276.
(44) Toh, R. J.; Evans, R.; Thissen, H.; Voelcker, N. H.; d'Ischia, M.; Ball, V. Deposition of Aminomalononitrile-Based Films: Kinetics, Chemistry, and Morphology. *Langmuir* **2019**, *35*, 9896−9903.
(45) Pracht, P.; Bohle, F.; Grimme, S. Automated exploration of the low-energy chemical space with fast quantum chemical methods. *Phys. Chem. Chem. Phys.* **2020**, *22*, 7169−7192.
(46) (a) Roy, D.; Najafian, K.; Schleyer, P. V. R. Chemical evolution: the mechanism of the formation of adenine under prebiotic conditions. *Proc. Natl. Acad. Sci. U. S. A.* **2007**, *104*, 17272−17277. (b) Glaser, R.; Hodgen, B.; Farrelly, D.; McKee, E. Adenine Synthesis in Interstellar Space: Mechanisms of Prebiotic Pyrimidine-Ring Formation of Monocyclic HCN-Pentamers. *Astrobiology* **2007**, *7*, 455−470. (c) Jung, S. H.; Choe, J. C. Mechanisms of Prebiotic Adenine Synthesis from HCN by Oligomerization in the Gas Phase. *Astrobiology* **2013**, *13*, 465−475.
(47) (a) Moffat, J. B. Three dimers of hydrogen cyanide: iminoacetonitrile, aminocyanocarbene, and azacyclopropenylidenimine; geometry-optimized Ab initio energies. *J. Chem. Soc., Chem. Commun.* **1975**, 888−890. (b) Freeman, F.; Gomarooni, M. Singlet−triplet gaps and insertion reactions of aminocyanocarbenes: A computational study of hydrogen cyanide covalent dimers. *Int. J. Quantum Chem.* **2006**, *106*, 2379−2389.
(48) Koch, D. M.; Toubin, C.; Xu, S.; Peslherbe, G. H.; Hynes, J. T. Concerted Proton-Transfer Mechanism and Solvation Effects in the HNC/HCN Isomerization on the Surface of Icy Grain Mntles in the Interstellar Medium. *J. Phys. Chem. C* **2007**, *111*, 15026−15033.
(49) Sandström, H.; Rahm, M. The Beginning of HCN Polymerization: Iminoacetonitrile Formation and Its Implications in Astrochemical Environments. *ACS Earth Space Chem.* **2021**, *5*, 2152−2159.
(50) Sandström, H.; Rahm, M. Crossroads at the Origin of Prebiotic Chemical Complexity: Hydrogen Cyanide Product Diversification. *J. Phys. Chem. A* **2023**, *127*, 4503−4510.
(51) Bannwarth, C.; Caldeweyher, E.; Ehlert, S.; Hansen, A.; Pracht, P.; Seibert, J.; Spicher, S.; Grimme, S. Extended tight-binding quantum chemistry methods. *WIREs Comput. Mol. Sci.* **2021**, *11*, No. e1493.
(52) Ehlert, S.; Stahn, M.; Spicher, S.; Grimme, S. Robust and Efficient Implicit Solvation Model for Fast Semiempirical Methods. *J. Chem. Theory Comput.* **2021**, *17*, 4250−4261.
(53) Becke, A. D. A new mixing of Hartree-Fock and local density-functional theories. *J. Chem. Phys.* **1993**, *98*, 1372−1377.
(54) Frisch, M. J.; Trucks, G. W.; Schlegel, H. B.; Scuseria, G. E.; Robb, M. A.; Cheeseman, J. R.; Scalmani, G.; Barone, V.; Petersson, G. A.; Nakatsuji, H.; Li, X.; Caricato, M.; Marenich, A. V.; Bloino, J.; Janesko, B. G.; Gomperts, R.; Mennucci, B.; Hratchian, H. P.; Ortiz, J. V.; Izmaylov, A. F.; Sonnenberg, J. L.; W-Y, D.; Ding, F.; Lipparini, F.; Egidi, F.; Goings, J.; Peng, B.; Petrone, A.; Henderson, T.; Ranasinghe, D.; Zakrzewski, V. G.; Gao, J.; Rega, N.; Zheng, G.; Liang, W.; Hada, M.; Ehara, M.; Toyota, K.; Fukuda, R.; Hasegawa, J.; Ishida, M.; Nakajima, T.; Honda, Y.; Kitao, O.; Nakai, H.; Vreven, T.; Throssell, K.; Montgomery, J. A., Jr.; Peralta, J. E.; Ogliaro, F.; Bearpark, M. J.; Heyd, J. J.; Brothers, E. N.; Kudin, K. N.; Staroverov, V. N.; Keith, T. A.; Kobayashi, R.; Normand, J.; Raghavachari, K.; Rendell, A. P.; Burant, J. C.; Iyengar, S. S.; Tomasi, J.; Cossi, M.; Millam, J. M.; Klene, M.; Adamo, C.; Cammi, R.; Ochterski, J. W.; Martin, R. L.; Morokuma, K.; Farkas, O.; Foresman, J. B.; Fox, D. J.. *Gaussian 16, Revision B.01*; Gaussian, Inc: Wallingford, CT, 2016.
(55) Grimme, S.; Ehrlich, S.; Goerigk, L. Effect of the damping function in dispersion corrected density functional theory. *J. Comput. Chem.* **2011**, *32*, 1456−1465.
(56) Tomasi, J.; Mennucci, B.; Cammi, R. Quantum Mechanical Continuum Solvation Models. *Chem. Rev.* **2005**, *105*, 2999−3093.
(57) Zhao, Y.; Truhlar, D. G. The M06 suite of density functionals for main group thermochemistry, thermochemical kinetics, noncovalent interactions, excited states, and transition elements: two new functionals and systematic testing of four M06-class functionals and 12 other functionals. *Theor. Chem. Acc.* **2008**, *120*, 215−241.
(58) (a) Kresse, G.; Furthmüller, J. Efficiency of ab-initio total energy calculations for metals and semiconductors using a plane-wave basis set. *Comput. Mater. Sci.* **1996**, *6*, 15−50. (b) Kresse, G.; Furthmueller, J. Efficient iterative schemes for ab initio total-energy calculations using a plane-wave basis set. *Phys. Rev. B* **1996**, *54*, 11169−11186.
(59) Kresse, G.; Joubert, D. From ultrasoft pseudopotentials to the projector augmented-wave method. *Phys. Rev. B: Condens. Matter Mater. Phys.* **1999**, *59*, 1758−1775.
(60) Togo, A.; Tanaka, I. First principles phonon calculations in materials science. *Scr. Mater.* **2015**, *108*, 1−5.

https://doi.org/10.1021/acsearthspacechem.4c00088
ACS Earth Space Chem. 2024, 8, 1272−1280